Derivative-State Analysis of a Sequential Intramolecular Vibrational Energy Re-distribution

Kiyohiko Someda

Department of Pure and Applied Sciences, Graduate School of Arts and Sciences, The University of Tokyo, Komaba, Meguro-ku, Tokyo 153

(Received March 22, 1996)

The Mori expansion adapted to pure-state dynamics is shown to be useful for analyzing a sequential intramolecular vibrational energy re-distribution (IVR). The expansion produces non-stationary basis states, "derivative states", which form a chain of mutually interacting quantum states beginning at a given initial state. An analysis based on this chain clearly demonstrates how the Hilbert space of quantum states is explored in sequential IVR. The derivative states can be classified into several "generations", and, thereby, a genealogy of quantum states can be discussed.

Analyses of the complex spectra of vibrationally highly excited molecules have revealed that the spectra sometimes possess a hierarchical structure, and that it is a reflection of the hierarchy of the molecular motions of different time scales.[1—6] In such a situation IVR (intramolecular vibrational energy re-distribution) occurs stepwise; the Hilbert space of the quantum states is explored sequentially. "Feature state" is a key concept in this topic;[6—14] it indicates a peak in a low-resolution spectrum, and has an approximate quantum number(s), which is good only for a certain short time scale. An overview of the recent experimental as well as theoretical studies on this topic can be found in Ref. 12. A complete understanding of IVR requires answers to the following questions:

(1) Which portion of Hilbert space has been explored up to a given time scale?

(2) How is the sequential exploration reflected in the spectrum?

(3) What are the wave functions of the feature states?

A key quantity that connects the dynamics with the optical spectra is the auto-correlation function, $K_{00}(t) = \langle \lambda^{(0)} | e^{-iHt/\hbar} | \lambda^{(0)} \rangle$, of the initial state, $|\lambda^{(0)}\rangle$, of an optical transition.[15—17] The Fourier transform of $K_{00}(t)$ is related to the Green function, $G_{00}^{(+)}(E)$, as[18]

$$iG_{00}^{(+)}(E) = \lim_{\varepsilon \to +0} i \left\langle \lambda^{(0)} \left| \frac{1}{E - H + i\varepsilon} \right| \lambda^{(0)} \right\rangle = \lim_{\varepsilon \to +0} \frac{1}{\hbar} \int_{-\infty}^{\infty} dt e^{i(E+i\varepsilon)t/\hbar} \theta(t) K_{00}(t), \quad (1)$$

where $\theta(t)$ is the step function. The absorption spectrum ($I(E)$) is obtained by the relation $I(E) \propto -ImG_{00}^{(+)}(E)$.[15—17] This correlation between the spectra and the dynamics, which originates from the uncertainty relation between the energy and time, is a key to understanding sequential IVR.

Based upon the above correlation between the spectra and the dynamics, an important study was made by M. J. Davis.[6,11,13] He discussed a hierarchical tree-structure of spectra based on a systematic smoothing procedure. In his method, a fully resolved spectrum is smoothed by a Gaussian window function with increasing width, and a tree diagram is drawn in accordance with the way the adjacent spectral peaks merge with each other. Due to the uncertainty relation between the energy and time, the hierarchical tree of a spectrum represents, at the same time, a pathway for exploring Hilbert space. Davis obtained the wave functions of smoothed states, which are nothing but feature states, by using linear combinations of the eigenstates. Davis thus gave a powerful tool for analyzing and understanding sequential IVR. Although Davis' scheme precisely grasps the essence of the issue, it has not been rigorously derived from quantum mechanics. In Davis' method, one does not refer to the Hamiltonian when one merges the adjacent spectral peaks to form a smoothed state. For completely non-integrable systems, this method is expected to give the correct results. For a system having constant(s) of motion, however, the adjacent eigenstates possibly belong to different branches of the hierarchical tree. The right partner can be located apart. For instance, when singlet and triplet manifolds overlap with each other in a certain system with a negligible spin-orbit interaction, the right partner is not always located adjacently, and hierarchical tree has to be drawn for each manifold. In such a case, needless to say, we know that the system has a good spin quantum number, and can easily draw hierarchical trees separately. A similar circumstance, however, can also arise in a system having approximate constant(s) of motion; in this case we cannot be aware of the existence of approximate constant(s) of motion harmful to the analysis before we carry it out. In summary, we need an alternative method based on quantum mechanics with mathematical rigor.

The present study aims to develop a rigorous quantum-mechanical method to analyze how Hilbert space can be explored in sequential IVR. For this purpose, the Mori expan-

sion is adopted in the present study. In the next section, we discuss why the exploration of Hilbert space is a useful point of view in an analysis of IVR, and why the Mori expansion is adopted for that purpose. In Section 2, the formulae of the Mori expansion adapted to pure state dynamics is briefly reviewed. In Section 3, the ground for truncating the Mori expansion is discussed. A prototypical model of sequential IVR is analyzed based on the Mori expansion in Section 4. The analysis clearly demonstrates how Hilbert space is explored in the course of time evolution. Truncation of the expansion is shown to give a good short-time approximation, and it properly reproduces the well-known correlation between the auto-correlation function and the spectrum. In Section 5, the present method is shown to be capable of producing the wave function of the feature state. In Section 6, a method is presented to construct a genealogy of quantum states which clarifies the nested structure of Hilbert space. Concluding remarks are presented in Section 7.

1. A Strategy for the Analysis of Sequential IVR. As mentioned in the preceding section, the feature state is a key concept for understanding sequential IVR. "To find a feature state" is synonymous with "to find an approximate constant of motion". As discussed in the literature,[2,12] anharmonic resonances are in many cases a key mechanism resulting in sequential dynamics. In such a case, a sum of integer multiples of the vibrational actions is an approximate constant of motion. Needless to say, the existence of approximate constants of motion (X) is ascribable to the Hamiltonian that allows a partition, $H=H^{(0)}+V$, where $H^{(0)}$ commutes with X. When the perturbation V is sufficiently small, the dynamics is governed by $H^{(0)}$, and X remains a good constant of motion on a certain short time scale. As discussed by Holme and Levine,[2] the Hamiltonian can be partitioned as $H=H^{(0)}+V^{(1)}+V^{(2)}+\cdots$, if the dynamics is sequential. Each member of the sequence $V^{(1)}$, $V^{(2)}$, $\cdots$ represents the interaction governing each rank of the hierarchy.

We must note that dyanmics depends on the initial state ($\phi^{(0)}$) as well as the Hamiltonian. An extreme example is the case in which $\phi^{(0)}$ is a linear combination of two eigenstates. In this case, the dynamics is a simple dephasing between those two states. If those eigenstates are complex linear combinations of the normal-mode basis, $H^{(0)}$ differs from the normal-mode Hamiltonian. For instance, when $\phi^{(0)}$ is a local mode-excited state, the short-time dynamics is governed by dephasing among the levels of a local mode multiplet. In this case, the proper $H^{(0)}$ is not the normal mode, but the local mode Hamiltonian. In short, the choice of $H^{(0)}$ is not trivial and depends on $\phi^{(0)}$. This point is a very central problem in the analysis of IVR.

Since the dynamics depends on $\phi^{(0)}$, it is useful to discuss the dynamics based not on the partition, $H=H^{(0)}+V$, but on the structure of the Hilbert space of the quantum states. In sequential IVR, Hilbert space is explored sequentially by the state vector of the system. On the shortest time scale, the system is confined to a certain domain; on the next shortest time scale, the system is liberated to a wider domain, and so on. Hilbert space is formed of a hierarchical nest of such domains. The innermost member of this nest should contain the initial state ($\phi^{(0)}$). For instance, the shortest time dynamics in ordinary IVR is dephasing among the feature states, and the corresponding domain of the Hilbert space is spanned by the feature states. In the next shortest time scale, the relevant Hilbert space is spanned by the feature states belonging to the next rank of hierarchy. Accordingly, the analysis of IVR has to follow the following process: (1) to detect the hierarchical nest of domains of the Hilbert space, (2) to assign what kind of quantum states belong to each domain, and (3) to know how much amplitudes those quantum states acquire at a given time. For this purpose, we need a certain kind of series expansion for generating a nest of the domains of the Hilbert space.

There are many kinds of perturbation expansions: the Rayleigh–Schrödinger and the Brillouin–Wigner expansions for bound states, the Neumann series (or the Born expansion), and the continued fraction expansion for the Faddeev equation for scattering problems. All of these perturbation expansions are based on the partition, $H=H^{(0)}+V$. It is emphasized again that we do not know the proper partition, $H=H^{(0)}+V$, a priori. In other words, we need a method which tells us a proper way to make the partition. This is a reason why the Mori expansion is adopted in the present study. The Mori expansion does not assume any partition of the Hamiltonian. It needs a starting projection operator. It is clear that for our purpose this projection operator should be chosen as the projector on $\phi^{(0)}$, i.e., $P^{(0)}=|\phi^{(0)}\rangle\langle\phi^{(0)}|$. Although Mori's formalism was originally designed for the operators in quantum Liouville space, it can be adapted to the pure state dynamics in Hilbert space.[21]

The Mori expansion is known to be a short-time expansion. For instance, it has been applied to an analysis of the resonance scattering of an electron impinged on molecules; the short-time dynamics of the trapped electron was found to be well described by the first several terms of the expansion.[24,25] The pure-state version of the Mori expansion is also expected to be useful in describing the short-time dynamics of IVR. As mentioned above, the starting projection operator should be chosen as $P^{(0)}=|\phi^{(0)}\rangle\langle\phi^{(0)}|$. As discussed in Section 2, the Mori expansion with such a choice of the starting projection operator is essentially equivalent to Wyatt's recursive residue generating method (RRGM)[22,23] based on the Lanczos tridiagonalization. The RRGM is a powerful tool for calculating spectral profiles broadened due to the interaction with dense dark states, and was successfully applied to overtone spectroscopy.[22,23,26] In the existing literature, the RRGM is mainly used as a computational tool to obtain the Green function. In the present study, however, particular attention is focused on a physical picture carried by the basis states generated in the expansion. These basis states form a chain of mutually interacting non-stationary states; this chain is directly associated with the hierarchical nest of domains of the Hilbert space discussed above. Those basis states are called "derivative states" because they are derived from the initial state successively by the time derivative of the precursor. In the next section we begin by reviewing the Mori

expansion adapted to pure-state dynamics.

2. A Chain of Derivative States and a Continued Fraction Expansion. Mori dealt with the correlation function (in the statistical mechanical sense) of a Heisenberg operator. Upon translation from the Liouville space of operators to the Hilbert space of quantum states, one can adapt Mori's theory to a pure state.[21] Since the following formalism is parallel to that of Mori,[20] the algebra of the derivation is omitted. One should also note the parallelism between the present formalism and the Lanczos tridigonalization of a matrix, which is known to be efficient to calculate auto-correlation functions and spectral profiles.[22,23,26,27]

The wave function evolved from $|\lambda^{(0)}\rangle$ is given by $|\lambda^{(0)}(t)\rangle = e^{-iHt/\hbar}|\lambda^{(0)}\rangle$. A key notion of the present formalism is the time derivative of $|\lambda^{(0)}(t)\rangle$ at $t=0$,

$$|\lambda^{(1)}\rangle = Q^{(0)}\left.\frac{d|\lambda^{(0)}(t)\rangle}{dt}\right|_{t=0} = -\frac{i}{\hbar}Q^{(0)}H|\lambda^{(0)}\rangle, \tag{2}$$

where $Q^{(0)}$ is the projection operator, which removes the component $|\lambda^{(0)}\rangle$, i.e., $Q^{(0)}=1-|\lambda^{(0)}\rangle\langle\lambda^{(0)}|$. The "derivative state", $|\lambda^{(1)}\rangle$, is the new component (orthogonal to $|\lambda^{(0)}\rangle$) growing in an infinitesimally short time. In other words, $|\lambda^{(1)}\rangle$ represents the most significant "doorway" state. By a similar procedure one can define a sequence of derivative states,

$$\begin{aligned}|\lambda^{(j)}\rangle &= Q^{(j-1)}\left[\frac{d}{dt}\exp[-iQ^{(j-2)}Ht/\hbar]|\lambda^{(j-1)}\rangle\right]_{t=0}\\ &= -\frac{i}{\hbar}Q^{(j-1)}H|\lambda^{(j-1)}\rangle \quad (\text{for } j=2,3,4,\cdots).\end{aligned} \tag{3}$$

Here, the projection operator, $Q^{(j-1)}$, is defined as

$$Q^{(j-1)} = 1 - \sum_{k=0}^{j-1}\frac{1}{S^{(k)}}|\lambda^{(k)}\rangle\langle\lambda^{(k)}|, \tag{4}$$

where $S^{(k)}=\langle\lambda^{(k)}|\lambda^{(k)}\rangle$. The projection operator, $Q^{(j-1)}$, in Eq. 3 has the effect of Schmidt orthogonalization, and, consequently, all of the derivative states are orthogonal to each other. The normalization of $\{|\lambda^{(j)}\rangle\}$ produces unitary basis,

$$|\phi^{(j)}\rangle = \frac{i^j}{\sqrt{S^{(j)}}}|\lambda^{(j)}\rangle \ (j=0,1,2,\cdots). \tag{5}$$

The factor i^j is introduced so that all of the $|\phi^{(j)}\rangle$'s are real if H and $|\lambda^{(0)}\rangle$ are real.

The auto-correlation function of the j-th order derivative state is defined as

$$K^{(j)}(t) = \langle\lambda^{(j)}|\exp[-iQ^{(j-1)}Ht/\hbar]|\lambda^{(j)}\rangle. \tag{6}$$

The corresponding Green function, $G^{(j)}(E)$, can be defined by the Fourier transform of $K^{(j)}(t)$, similar to Eq. 1. The Green function $G^{(0)}(E)\equiv G_{00}^{(+)}(E)$ is shown to be written as the continued fraction expansion,

$$G^{(0)}(E) = \cfrac{\hbar S^{(0)}}{E-E^{(0)}-\cfrac{S^{(1)}}{-S^{(0)}}\cfrac{\hbar^2}{E-E^{(1)}-\cfrac{S^{(2)}}{-S^{(1)}}\cfrac{\hbar^2}{E-E^{(2)}-\cdots\cfrac{S^{(J)}}{-S^{(J-1)}}\cfrac{\hbar^2}{E-E^{(J)}-\hbar G^{(J+1)}(E)/S^{(J)}}}}} \tag{7}$$

where $E^{(j)}=\langle\phi^{(j)}|Q^{(j-1)}H|\phi^{(j)}\rangle$. It can be shown that the Hamiltonian matrix is tridiagonal in the derivative state representation, i.e.,

$$\langle\phi^{(k)}|H|\phi^{(j)}\rangle = E^{(j)}\delta_{k,j} + \hbar\sqrt{S^{(j+1)}/S^{(j)}}\,\delta_{k,j+1} + \hbar\sqrt{S^{(j)}/S^{(j-1)}}\,\delta_{k,j-1}. \tag{8}$$

This equation indicates that the derivative states are equivalent to the basis generated in the Lanczos tridiagonalization. In the present study, besides the numerical efficiency of the latter method, particular attention is focused on a physical picture carried, or generated, by the derivative states, themselves. As indicated by Eq. 8, the derivative states form a chain of mutually interacting non-stationary states beginning at the initial state $|\lambda^{(0)}\rangle$ as

$$|\lambda^{(0)}\rangle = |\phi^{(0)}\rangle \overset{\hbar\sqrt{S^{(1)}/S^{(0)}}}{\longleftrightarrow} |\phi^{(1)}\rangle \overset{\hbar\sqrt{S^{(2)}/S^{(1)}}}{\longleftrightarrow} |\phi^{(2)}\rangle \longleftrightarrow \cdots. \tag{9}$$

The derivative states are accessed one by one in the order of increasing j; i.e., they are arranged in the order of the exploration of Hilbert space, as will be shown in the example given in Section 4. In short-time dynamics, since not all of the derivative states participate, truncation of the chain (9) is expected to be efficient. This point is discussed in the next section.

Although the one-dimensional initial subspace $P^{(0)}\equiv|\lambda^{(0)}\rangle\langle\lambda^{(0)}|$ is assumed in the present paper, the original Mori theory has no such restriction. The above formalism can be extended to treat a multi-dimensional $P^{(0)}$, i.e., to treat a plural number of states at each step of the expansion.

3. A Low-Resolution Spectrum and a Short-Time Approximation. Neglecting the off-diagonal element, $\hbar\sqrt{S^{(J+1)}/S^{(J)}}$, of the tridiagonal Hamiltonian given in Eq. 8 leads to a truncated continued fraction (see Eq. 7), i.e., the $(J, J+1)$-Pade approximant for $G^{(0)}(E)$,

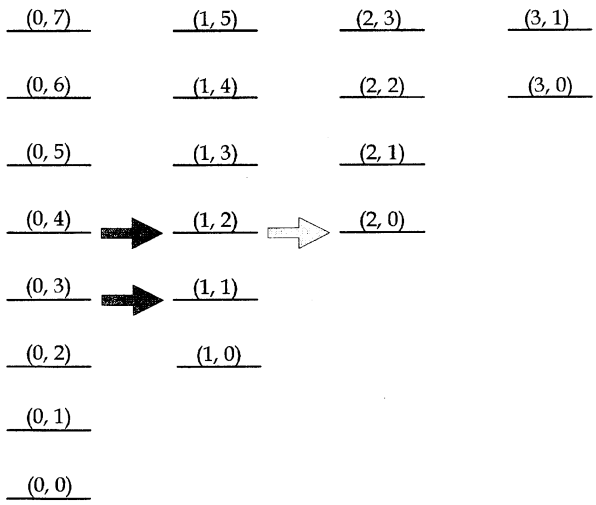

Fig. 1. The energy levels of the unperturbed 1 : 2 resonance Hamiltonian, i.e., H given in Eq. 11 with $\zeta=0$. The arrows indicate resonance energy transfer expected to occur in the case of weak coupling, i.e., the case of a small ζ.

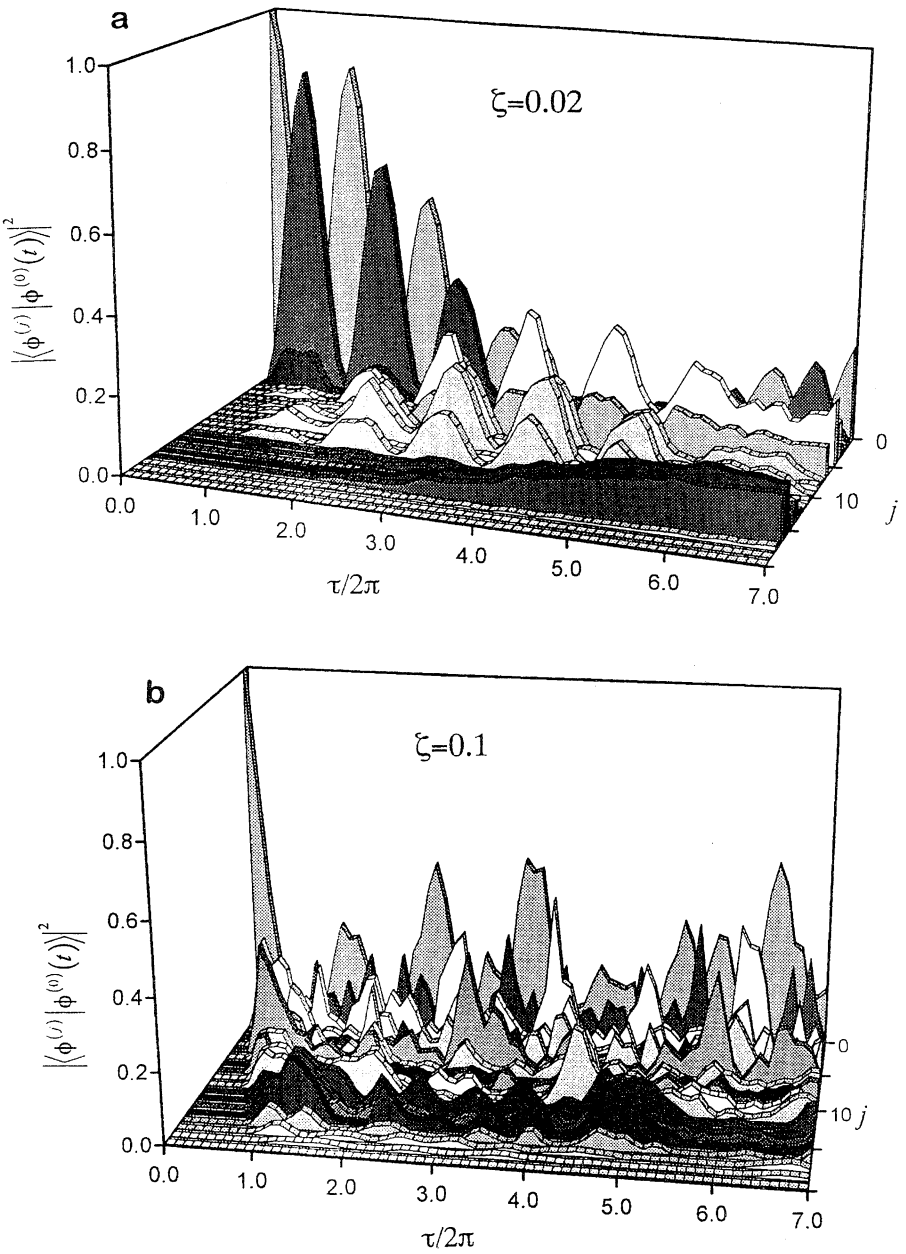

Fig. 2. The squared moduli of the auto- and mutual-correlation functions between the initial states and the derivative states, $|\langle\phi^{(j)}|\phi^{(0)}(t)\rangle|^2$ (j=0, 1, 2, ⋯), of the model presented in Section 4. a) the case of ζ=0.02. It is seen that the dynamics is sequential. b) the case of ζ=0.1. The dynamics is seen to be instantaneous.

$$G_J^{(0)}(E) = \frac{\hbar S^{(0)}}{E-E^{(0)}} \frac{S^{(1)}}{-S^{(0)}} \frac{\hbar^2}{E-E^{(1)}} - \cdots \frac{S^{(J)}}{-S^{(J-1)}} \frac{\hbar^2}{E-E^{(J)}} = \frac{A_J(E)}{B_J(E)}. \quad (10)$$

Here, $A_J(E)$ and $B_J(E)$ can be calculated using the well-known recursive equations, which are the J-th and $(J+1)$-st order polynomials of E, respectively.[28] As can be seen from Eq. 7, truncation of the continued fraction is justified when $|\hbar G^{(J+1)}(E)/S^{(J)}| \ll |E-E^{(J)}|$. Since the quantity $G^{(J+1)}(E)$ is the Green function of the subspace $Q^{(J)}$, it has poles on the real E-axis. Therefore, we cannot expect that the above inequality be fulfilled. In other words, it is difficult to clarify the convergence condition of the expansion, because $G^{(J+1)}(E)$ has a singularity. We must discuss the spectral profile with a finite resolution instead of the singular function $G_J^{(0)}(E)$. For low-resolved spectra, the truncation is verified as follows: Since the denominator of $G_J^{(0)}(E)$ in Eq. 10 is the J-th order polynomial, a finer structure of $G^{(0)}(E)$ is reproduced with increasing J. If the energy resolution is finite, the continued fraction is expected to converge at finite J. The spectrum with resolution γ is given by $-ImG^{(0)}(E+i\gamma)$. The truncation of the continued fraction expansion is justified when $|\hbar G^{(J+1)}(E+i\gamma)/S^{(J)}| \ll |E-E^{(J)}+i\gamma|$. In this case, the singularity of $G^{(J+1)}(E)$ is avoided. Roughly speaking, this is attained if $\hbar S^{(J+1)}/S^{(J)} \ll \gamma$. The Fourier transform of $G_J^{(0)}(E)$ gives a short-time approximation of $K_{00}(t)$ good for $t \ll \hbar/\gamma$. It should be noted that when the Hamiltonian is a matrix of finite size

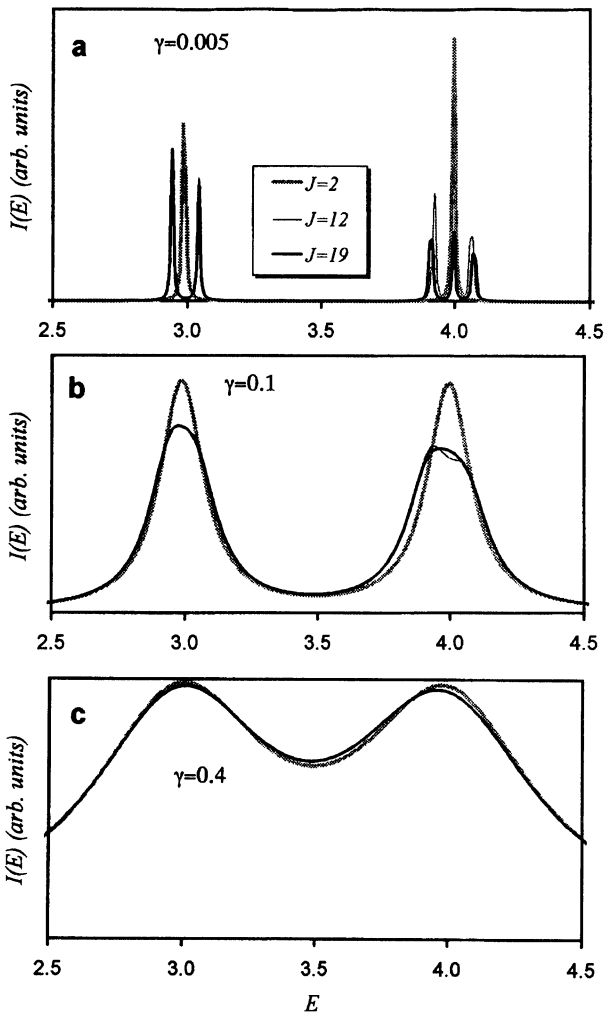

Fig. 3. Spectra of the model in Section 3. a) A high resolution spectrum with γ=0.005. The exact one with J=19 exhibits doublet and triplet peaks corresponding to the groups of states with v_+=3 and v_+=4, respectively. b) The low resolution spectrum with γ=0.1. J=12 suffices to reproduce the profile of the left doublet peak. c) The low resolution spectrum with γ=0.4. The cut-off order J=3 suffices to reproduce the spectral profile. Two broad peaks correspond to the feature states $|v_+=3\rangle$ and $|v_+=4\rangle$.

(N), the continued fraction terminates at the ($N-1$)-st order, and $G^{(0)}_{N-1}(E)$ is equal to the exact Green function.

4. An Example from a Coupled-Oscillator Having 1 : 2 Resonance. Analyses of the complex spectra of vibrationally highly excited molecules (acetylene[7–9] and nitrogen dioxide[29]) have shown that anharmonic resonance is a key to understanding the dynamics and spectra. The feature states and the separation of the time scale originate from the resonance. We discuss here a prototypical Hamiltonian of a two-dimensional coupled-oscillator in a 1 : 2 resonance, i.e.,

$$H = 2\omega a^+a + \omega b^+b + \zeta(a+a^+)(b+b^+)^2, \qquad (11)$$

where a and b are boson annihilation operators. The harmonic oscillator eigen-states, $|v_a v_b\rangle$, are used for the basis. The parameters are ω=1.0 and ζ=0.02. The units are chosen

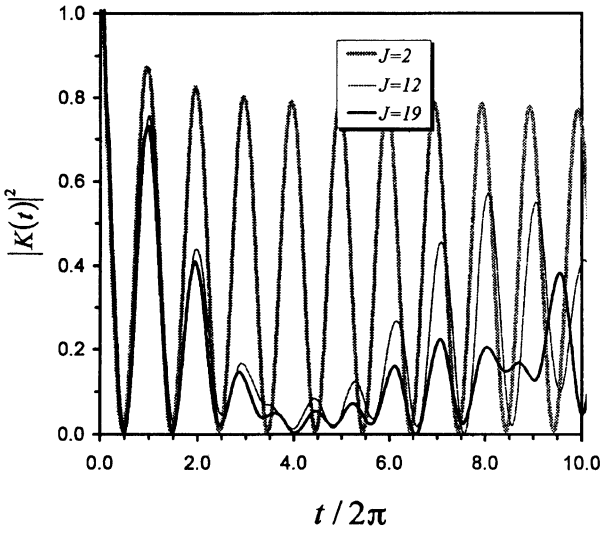

Fig. 4. The squared modulus of auto-correlation function of the model in Section 3. The case of J=19 gives the exact one. The auto-correlation functions with J=2 and 12 are seen to be short-time approximations.

so that $\hbar$=1. The lowest 20 basis states, $|v_a v_b\rangle$, are taken into account. The initial state is set as $|\phi^{(0)}\rangle=(|0,3\rangle+|0,4\rangle)/\sqrt{2}$. The unperturbed (i.e., ζ=0) energy levels are shown in Fig. 1. In the present model, $v_+=2v_a+v_b$, is the approximate quantum number. The feature state $|v_+=3\rangle$ is composed of $|0,3\rangle$ and $|1,1\rangle$, while the feature state $|v_+=4\rangle$ has three components: $|0,4\rangle$, $|1,2\rangle$, and $|2,0\rangle$.

Figure 2a displays time profiles of the squared moduli of the auto- and mutual-correlation functions, $|K_{j0}(t)|^2\equiv|\langle\phi^{(j)}|\phi^{(0)}(t)\rangle|^2$ (j=0, 1, 2,$\cdots$). These correlation functions are obtained from the exact energy eigenvalues and eigenfunctions. Figure 2a clearly demonstrates a useful property of the derivative states: They are accessed in the order of increasing j; thus, Fig. 2a visualizes how $|\phi^{(0)}(t)\rangle$ explores the Hilbert space of the derivative states during the course of time evolution. Furthermore, an intriguing phenomenon is seen. While the components $|\phi^{(1)}\rangle$ and $|\phi^{(2)}\rangle$ grow immediately at t=0, the components $|\phi^{(3)}\rangle-|\phi^{(11)}\rangle$ (the lightly shaded graphs in Fig. 2a) appear after a finite delay at $t/2\pi$=0.7; after a longer delay the components $|\phi^{(12)}\rangle-|\phi^{(16)}\rangle$ (the darkly shaded graphs) grow. In other words, there are gaps in the appearance times of the derivative states. These gaps are nothing but a reflection of sequential IVR. Based on these gaps one can classify the derivative states into "generations". The first generation, $\{|\phi^{(0)}\rangle$, $|\phi^{(1)}\rangle$, $|\phi^{(2)}\rangle\}$, includes components of the initial state, $|0,3\rangle$ and $|0,4\rangle$. The second generation, $\{|\phi^{(3)}\rangle-|\phi^{(11)}\rangle\}$, includes the basis states $|1,1\rangle$ and $|1,2\rangle$, while the third generation, $\{|\phi^{(12)}\rangle-|\phi^{(16)}\rangle\}$, includes $|2,0\rangle$. The appearances of the second and third generations exactly correspond to the resonance energy transfer by $\Delta v_a=-\Delta v_b/2$=1, and 2, respectively, as illustrated by the arrows in Fig. 1. The "generation-gaps" indicate that the energy transfer, i.e., IVR, takes place sequentially. On the other hand, Fig. 2b displays the case of a larger coupling constant, ζ=0.1. Although the derivative

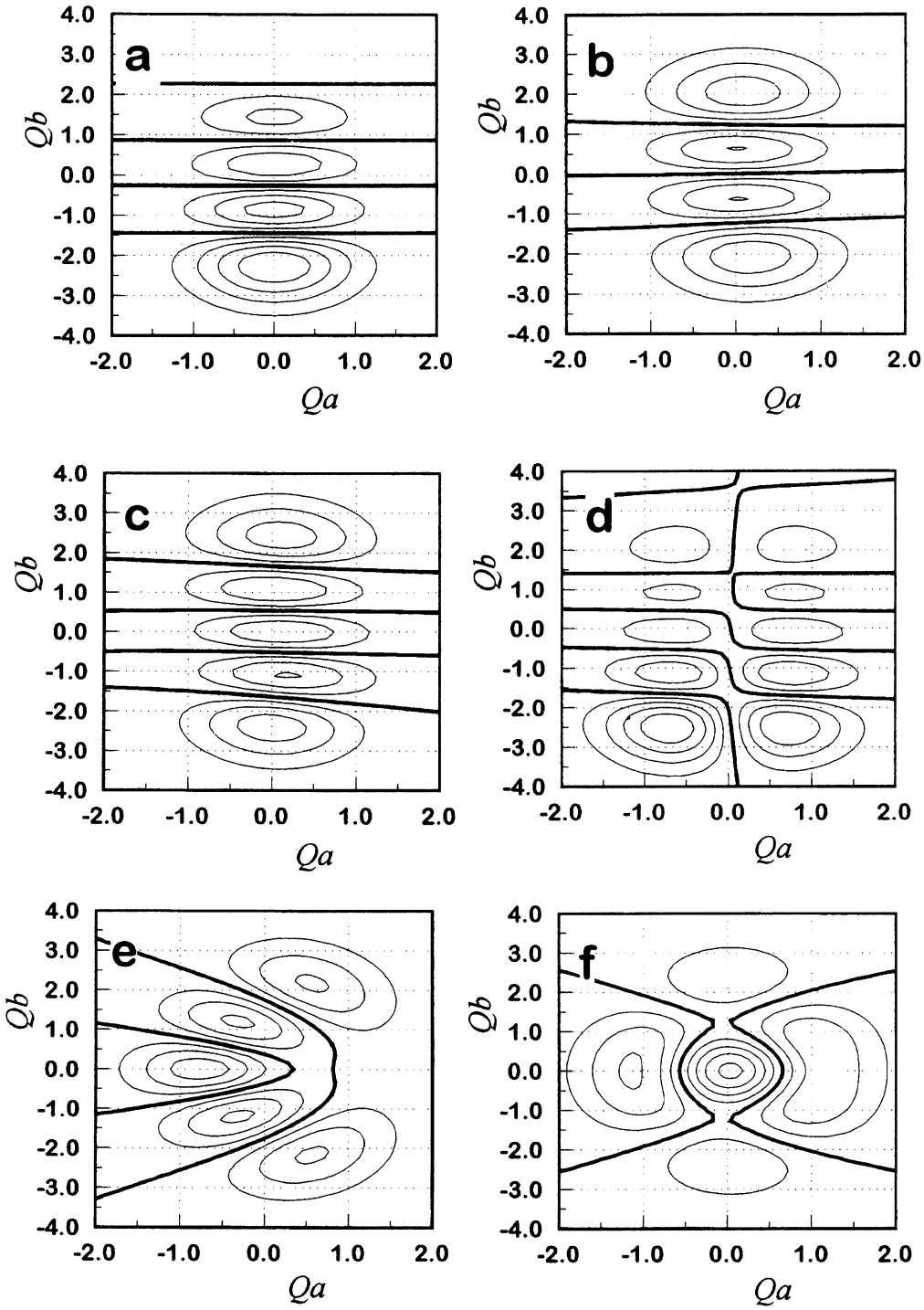

Fig. 5. a): A contour map of the wave function of the initial state. Thick lines represent the nodal lines. b), c), and d): The eigenfunctions of the 3×3 effective Hamiltonian for the short time dynamics. The method of obtaining them is given in Section 5. The main components of the wave functions in panels b), c), and d) are $|0,3\rangle$, $|0,4\rangle$, and $|1,4\rangle$, respectively, and their energy expectation values are 2.99, 4.00, and 6.14, respectively. The wave functions in panels b) and c) are interpreted as those of the feature states. e) and f): The wave functions of the eigenstates of the full Hamiltonian. Two members of the triplet $\{|0,4\rangle,|1,2\rangle,|2,0\rangle\}$ of the 1 : 2 resonance are shown. The wave functions of the other member is, roughly speaking, mirror image of panel e) with respect to Q_a=0 line.

states are seen to be accessed in the order of increasing j, there are no gaps in the appearance times. This indicates that IVR is instantaneous when ζ=0.1. The spectrum of the latter case (ζ=0.1) is found to exhibit no feature-state structure, while in the case of ζ=0.02 the spectrum does, as is discussed below.

Figure 3a displays the high-resolution spectra (γ=0.005) of the weak-coupling case (ζ=0.02) obtained from the con-

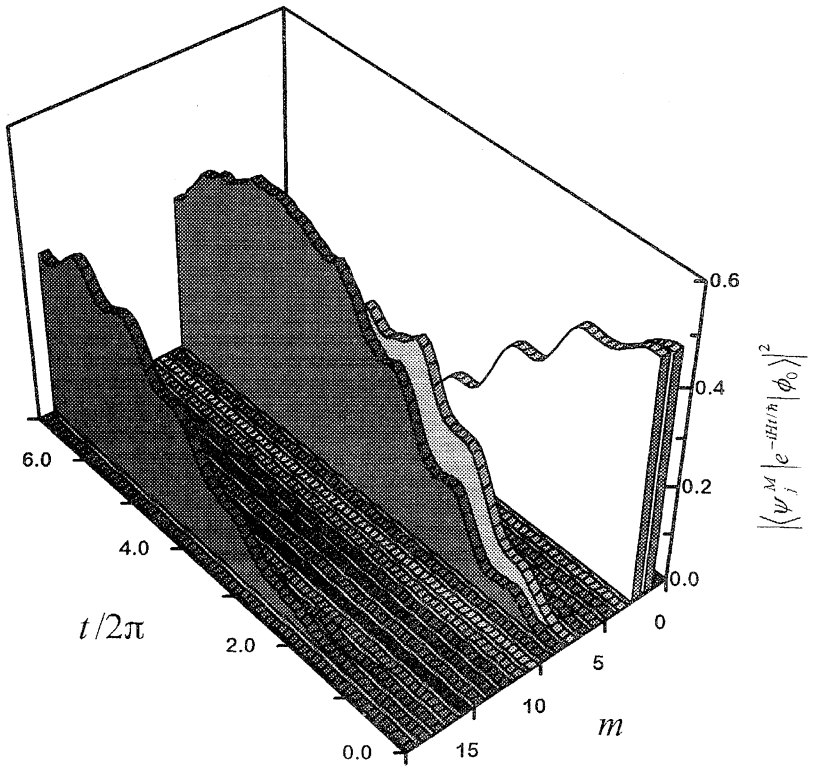

Fig. 6. The squared modulus of the mutual correlation function between the initial state and a generation-eigenstate, $|K_j^{(M)}|^2 = |\langle\psi_j^M|e^{-iHt/\hbar}|\phi_0\rangle|^2$, of the model in Section 4. Indices m=0, 1, 2,⋯, 19 indicate the generation-eigenstates $|\psi_1^I\rangle$, $|\psi_2^I\rangle$, $|\psi_3^I\rangle$, $|\psi_1^{II}\rangle$,⋯, $|\psi_9^{II}\rangle$, $|\psi_1^{III}\rangle$,⋯, $|\psi_8^{III}\rangle$, respectively. Details of the generation-eigenstate are given in Section 5.

tinued fractions with different cut-off orders. The spectrum with the cut-off order J=2 exhibits two peaks of the feature states. With increasing J, a splitting of the feature state-peaks appears. The spectrum with J=19, the exact one within the basis states used, shows all of the components of the feature states. Figures 3b and 3c display the spectra with lower resolutions. For instance, with γ=0.4, J=2 suffices to reproduce the profile of the two feature states. Figure 4 displays approximate auto-correlation functions together with the exact one, $K_{00}(t)$. The case of J=2 gives a good approximation during the earliest time scale $t/2\pi<0.7$, while the case of J=12 remains good for a later time.

Based upon the sequential dynamics of the weak-coupling model and the short-time approximation for it, wave functions of the feature states and a genealogy of quantum states are discussed in the following sections.

5. Wave Functions of Feature States. In quantum mechanics, a bound state can be identified as a pole of the Green function; this pole causes a spectral peak. When IVR is sequential, as can be seen in Fig. 2a, the feature states can be identified as poles of the approximate Green function obtained from the truncated continued fraction, i.e., the short-time apporximation. As discussed in the preceding section, the cut-off order J=2 suffices to reproduce the two feature state-peaks of the model system given in Eq. 11. The corresponding Green function, $G^{(2)}(E)$, has three poles. This implies that the dynamics of the shortest time scale can be approximately described by the three-state system of the first generation $\{|\phi^{(0)}\rangle, |\phi^{(1)}\rangle, |\phi^{(2)}\rangle\}$. The eigenvalues of the corresponding 3×3 Hamiltonian are nothing but the three poles of $G^{(2)}(E)$. Two of those eigenvalues are interpreted as being the energy positions of the feature states, and the corresponding eigenvectors give the wave functions of the feature states. The remaining one state takes the role of adjusting the energy positions of the feature states.

The eigenfunctions of the 3×3 Hamiltonian were calculated, and are shown in Fig. 5 together with the initial wave function and several of the eigenfunctions of the full Hamiltonian. Panels **b**, **c**, and **d** show the eigenfunctions of the 3×3 Hamiltonian, $|\psi_3^I\rangle$, $|\psi_2^I\rangle$, and $|\psi_1^I\rangle$, respectively. The main component of $|\psi_3^I\rangle$ is $|0,3\rangle$, as indicated by its nodal structure, while $|\psi_2^I\rangle$ mainly composes $|0,4\rangle$. These two states can be interpreted as the feature states. Although the wave functions of $|\psi_3^I\rangle$ and $|\psi_2^I\rangle$ resemble those of the 0-th order basis, $|0,3\rangle$ and $|0,4\rangle$, the former wave functions are no longer symmetric with respect to the inversion of the vibrational coordinate, $Q_a \rightarrow -Q_a$ (where $Q_a \equiv (2\omega)^{-1/2}(a^+ + a)$). This is due to the anharmonicity of the system: Some of the anharmonic coupling among the 0-th order basis is working in the short-time dynamics, and its effect is brought into the wave functions of the feature states, $|\psi_3^I\rangle$ and $|\psi_2^I\rangle$. In short, the wave functions of $|\psi_3^I\rangle$ and $|\psi_2^I\rangle$ differ from the 0-th order basis, $|0,3\rangle$ and $|0,4\rangle$, because of the anharmonicity. The remaining state, $|\psi_1^I\rangle$, takes a role of bringing the effect of anharmonicity into the 3×3 Hamiltonian of the first generation. Figures 5e and 5f display the eigenfunctions of

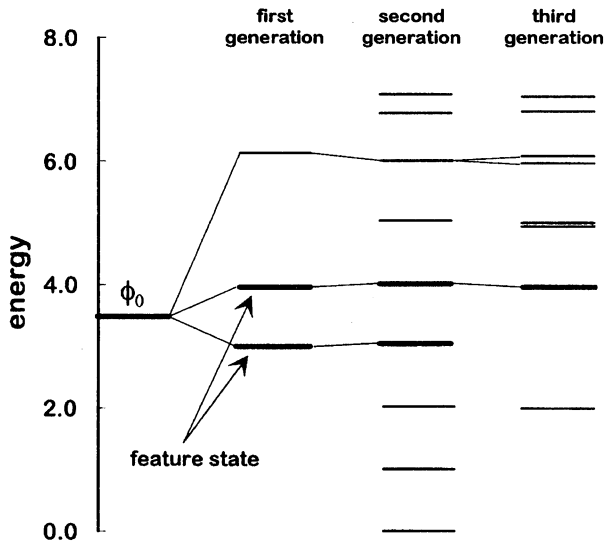

Fig. 7. The genealogy of the generation-eigenstates. The generation-eigenstates $|\psi_j^M\rangle$ of the three generations are represented by the energy levels placed at their energy expectation values. The energy level indicated as ϕ_0 represents the initial state. The generation-eigenstates which have substantial amplitude are indicated by thick energy levels. The successor-state is identified by examining the magnitude of coupling given in Eq. 12, i.e., the member of the succeeding generation that has the largest coupling is assigned as the successor and linked by a line in the figure.

the full Hamiltonian. They have a nodal structure typical to a coupled oscillator in resonance, and its topology differs totally from that of the feature states. It should be noted that the wave functions of the feature states depend on the initial state. A feature state can be interpreted as being degenerate. For instance, the feature state $|\nu_+=4\rangle$ is triply degenerate in the present model. Among the degenerate components, the component closest to the initial state is selected in the wave function of the feature state in Fig. 5c.

6. A Genealogy of Quantum States. The time profile of IVR is best understood by a "tree" structure of non-stationary states[6,10,11,13,14,30] rather than a one-dimensional chain. That is to say, "branching" is significant in understanding a genealogy. As discussed in Section 4, the chain of the derivative states serves to detect the generations of the quantum states. Within a generation, however, the derivative states exhibit dephasing, as is shown in Fig. 2a. By re-organizing the derivative states within a given generation, one can clarify which state actually carries the population, i.e., who succeeded heritage of precursors. The diagonalization of the 3×3 Hamiltonian to obtain the feature states in the preceding section was a procedure aimed at this purpose. Similarly, diagonalization of the Hamiltonian within the subspaces of the succeeding generations serves to clarify the genealogy of the quantum states.

The eigenstates of the subspaces of three generations, i.e., $\{|\phi^{(0)}\rangle-|\phi^{(2)}\rangle\}$, $\{|\phi^{(3)}\rangle-|\phi^{(11)}\rangle\}$, and $\{|\phi^{(12)}\rangle-|\phi^{(19)}\rangle\}$, were calculated. The thus-obtained "generation-eigenstates" are denoted as $|\psi_j^M\rangle$, where M indicates the generation (M=I, II, and III) and j represents the numbering within a given generation. The mutual correlation function between a generation-eigenstate and the initial state, $K_j^{(M)}\equiv\langle\psi_j^M|e^{-iHt/\hbar}|\phi_0\rangle$, was calculated, and is shown in Fig. 6. Figure 6 looks very different from Fig. 2a in that only a few selected generation-eigenstates have substantial amplitudes. This is because the generation-eigenstates have less energy uncertainty than do the derivative states, and dephasing within the generation is suppressed. Figure 6 clearly shows that two members of the first generation, $|\psi_2^I\rangle$ and $|\psi_3^I\rangle$ (the white graphs), carried on almost all of the heritage from the initial state. At $t/2\pi$=0.5, two members of the second generation, $|\psi_5^{II}\rangle$ and $|\psi_6^{II}\rangle$ (the shaded graphs at m=7 and 8 in Fig. 6), begin to accept the heritage from the first generation, and, then, transfer it to one member of the third generation, $|\psi_7^{III}\rangle$ (the shaded graph at m=18 in Fig. 6), at $t/2\pi$=2.0. Figure 6 also shows that many of the generation-eigenstates are not actually populated. This is because the energy spectra of those states does not overlap with the energy spectrum of the initial state. Those states are "virtual" states, which work to bring the effect of anharmonicity into the wave functions of the "successors of heritage".

In order to make a genealogy of the generation-eigenstates, one must know who is the successor of a given state. The generation-eigenstates have no coupling within the same generation, but have it with the precursor(s) and the successor(s). The successor(s) can be identified by examining the magnitude of the coupling. A possible measure of the magnitude of the coupling is the coefficient of the first-order Rayleigh–Schrödinger perturbation,[26]

$$C_{j,k}^{M,M+1}\equiv\frac{\langle\psi_j^M|H|\psi_k^{M+1}\rangle}{\langle\psi_j^M|H|\psi_j^M\rangle-\langle\psi_k^{M+1}|H|\psi_k^{M+1}\rangle}. \qquad (12)$$

By examining the above coefficients, a genealogy of the generation-eigenstates is constructed (Fig. 7). This diagram of genealogy illustrates who carried on the heritage of the amplitude originating from the initial state. Figure 7 exactly reproduces a picture of the resonance-energy transfer mentioned in Section 3.

7. Concluding Remarks. Through the example presented in Section 4, it can be seen that the derivative states are useful for detection of sequential dynamics. This is due to the property of the derivative states, in that they are accessed in accordance with their order (j). The derivative states of the lower order are relevant with the short-time dynamics. Thus, one can extract the portion of Hilbert space significant to short-time dynamics. Low-resolution spectra can be obtained from that portion of Hilbert space, i.e., the lower order derivative states. The eigenstates of the Hamiltonian projected on that portion of Hilbert space are interpreted as feature states. One can define the generation of derivative states if the dynamics is sequential. The generation-eigenstates, the eigenstates of the subspace of a given generation, are useful for discussing the genealogy of the quantum states participating in IVR.

Based on the subspaces of the generation, the partition of the Hamiltonian discussed in Section 1 can be carried out.

By using the projection operator onto each generation,

$$\Pi^{(M)} = \sum_j |\psi_j^{(M)}\rangle\langle\psi_j^{(M)}|, \tag{13}$$

the Hamiltonian can be written as

$$H = H^{(0)} + V^{(1)} + V^{(2)} + \cdots, \tag{14}$$

where

$$H^{(0)} = \Pi^{(I)} H \Pi^{(I)} \tag{15}$$

and

$$V^{(M)} = \Pi^{(M)} H \Pi^{(M)} + \Pi^{(M)} H \Pi^{(M-1)} + \Pi^{(M-1)} H \Pi^{(M)} \tag{16}$$

This is exactly the partition discussed by Holme and Levine.[2] In short, the present method is shown to be capable of deriving the partition of a given Hamiltonian which describes the sequential dynamics without postulating any $H^{(0)}$ a priori.

The diagram of the genealogy in the present paper differs from the "tree" diagram given in the literature;[6,10,11,13,14,30] the former belongs to a type of "tier" diagram of A. Stucheburkhov.[26] By using the sets of eigenstates of $H^{(0)}$, $H^{(0)}+V^{(1)}$, $H^{(0)}+V^{(1)}+V^{(2)}$, however, we can construct a tree diagram of the spectrum. Those eigenstates are essentially, or in other words, conceptually, the same as Davis' smoothed states.[6,11,13] The wave function of the feature states obtained in the present method is also essentially the same as those of Davis. In short, the present method is capable of producing useful concepts originally devised by Davis. As discussed in introduction, Davis' method, though it is useful conceptually, has shortcomings in that it is not completely based on rigorous quantum mechanics. It is emphasized that the present method is derived from completely rigorous dynamics. It should also be noted that Stucheburkhov's tier diagram is generated based on the first-order Rayleigh–Schrödinger perturbation, while the present analysis is based on the exact dynamics in detecting the generations of the quantum states.

The expansion employed in the present work is essentially equivalent with Wyatt's RRGM in that both methods are based on the Lanczos method. Regarding the details, however, both methods differ from each other. In the RRGM, the initial-state vector of the Lanczos algorithm is set as $|u\rangle=(|i\rangle+|f\rangle)/\sqrt{2}$, where $|i\rangle$ and $|f\rangle$ are the initial and the final states of interest. The so-called u-chain is derived from $|u\rangle$ by the Lanczos recursion. At the same time, the v-chain is calculated starting from $|v\rangle=(|i\rangle-|f\rangle)/\sqrt{2}$. The correlation functions are obtained by using information from both chains. The method employed in the present study is simpler. The Lanczos recursion is started from the initial state, $|\phi^{(0)}\rangle$. The chain state, called the derivative state in the present paper, obtained from the latter recursion, is found to have a useful physical picture directly connected with sequenital dynamics, while Wyatt et al. have discussed little about the physical contents of the u- and v-chains.

The points left for a future study are as follows: (i) Measures of the volume of Hilbert space (or phase space) explored up to a given time have been proposed in the literature.[4,31] Figure 2a implies that the number of derivative states accessed up to a given time can also be an alternative measure. (ii) Gaps in appearance times should be predicted from $S^{(j+1)}/S^{(j)}$ and $E^{(j)}$ of the chain scheme (9). The example in Section 4 suggests that the gaps do not simply indicate small $S^{(j+1)}/S^{(j)}$ at the corresponding j. It is necessary to clarify the cooperative effect of $S^{(j+1)}/S^{(j)}$ and $E^{(j)}$ on the dynamics. (iii) In the present paper, one constructs the one-dimensional chain of the derivative states at first, and then converts it to the tier-diagram in order to discuss the genealogy of the generation-eigenstates. By using the multidimensional version of the Mori formalism mentioned in the final paragraph of Section 2, there is a possibility to directly detect "tree" structure of the quantum states.

The present study was started when the author stayed at the Fritz Haber Research Center for Molecular Dynamics, the Hebrew University of Jerusalem. The author is grateful to Professor Raphael D. Levine for stimulating discussions. The present study was supported by a grant under the Japan–Israel International Scientific Research Program and a Grant-in-Aid for Scientific Research, both from the Ministry of Education, Science and Culture of Japan.

References

1) R. L. Sundberg, E. Abramson, J. L. Kinsey, and R. W. Field, *J. Chem. Phys.*, **83**, 466 (1985).
2) T. A. Holme and R. D. Levine, *Chem. Phys.*, **131**, 169 (1989).
3) J. C. Lorquet, Y. M. Engel, and R. D. Levine, *Chem. Phys. Lett.*, **175**, 461 (1990).
4) F. Remacle and R. D. Levine, *Chem. Phys. Lett.*, **181**, 307 (1991).
5) F. Remacle and R. D. Levine, *J. Chem. Phys.*, **98**, 2144 (1993).
6) M. J. Davis, *J. Chem. Phys.*, **98**, 2614 (1993).
7) K. Yamanouchi, N. Ikeda, S. Tsuchiya, D. M. Jonas, J. K. Lundberg, G. W. Adamson, and R. W. Field, *J. Chem. Phys.*, **95**, 6330 (1991).
8) D. M. Jonas, S. A. B. Solina, B. Rajaram, R. J. Silbey, R. W. Field, K. Yamanouchi, and S. Tsuchiya, *J. Chem. Phys.*, **97**, 2813 (1992).
9) D. M. Jonas, S. A. B. Solina, B. Rajaram, R. J. Silbey, R. W. Field, K. Yamanouchi, and S. Tsuchiya, *J. Chem. Phys.*, **99**, 7350 (1994).
10) R. W. Field, S. L. Coy, and S. A. B. Solina, *Prog. Theor. Phys., Suppl.*, **116**, 143 (1994).
11) M. J. Davis, *Int. Rev. Phys. Chem.*, **14**, 15 (1995).
12) H.-L. Dai and R. W. Field, "Molecular Dynamics and Spectroscopy by Stimulated Emission Pumping," World Scientific, Singapore (1995).
13) M. J. Davis, Chapter 23 of Ref. 12.
14) S. L. Coy, D. Chasman, and R. W. Field, Chapter 24 of Ref. 12.
15) E. J. Heller, *Acc. Chem. Res.*, **14**, 368 (1981).
16) S. Y. Lee and E. J. Heller, *J. Chem. Phys.*, **71**, 4777 (1979).
17) E. J. Heller, R. L. Sundberg, and D. J. Tannor, *J. Phys. Chem.*, **86**, 267 (1993).
18) For example, see : R. D. Levine, "Quantum Mechanics of Molecular Rate Processes," Oxford University Press, Oxford

(1965).
19) H. Mori, *Prog. Theor. Phys.*, **33**, 423 (1965).
20) H. Mori, *Prog. Theor. Phys.*, **34**, 399 (1965).
21) K. Someda and R. D. Levine, *Chem. Phys.*, **184**, 187 (1994).
22) R. E. Wyatt, *Adv. Chem. Phys.*, **73**, 231 (1989).
23) C. Leforestier and R. E. Wyatt, Chapter 21 of Ref. 12.
24) H. Estrada and W. Domcke, *Phys. Rev. A*, **A40**, 1262 (1989).
25) W. Domcke, *Phys. Rep.*, **208**, 97 (1991).
26) A. A. Stuchebrukhov and R. A. Marcus, *J. Chem. Phys.*, **98**, 6044 (1993).
27) H. Kono, *Chem. Phys. Lett.*, **214**, 137 (1993).
28) G. A. Baker, Jr., "Essentials of Pade Approximants," Academic Press, New York (1975).
29) J. Miyawaki, K. Yamanouchi, and S. Tsuchiya, *J. Chem. Phys.*, **99**, 254 (1993).
30) D. E. Logan and P. G. Wolynes, *J. Chem. Phys.*, **93**, 4994 (1990).
31) E. J. Heller, *Phys. Rev. A*, **A35**, 1360 (1987).